NASA TECHNICAL NOTE

NASA TN D-3909

NASA TN D-3909

A FLIGHT AND SIMULATOR STUDY OF DIRECTIONAL AUGMENTATION CRITERIA FOR A FOUR-PROPELLERED STOL AIRPLANE

by Hervey C. Quigley, Robert C. Innis, Richard F. Vomaske, and Jack W. Ratcliff

Ames Research Center
Moffett Field, Calif.

NATIONAL AERONAUTICS AND SPACE ADMINISTRATION • WASHINGTON, D. C. • MAY 1967

NASA TN D-3909

A FLIGHT AND SIMULATOR STUDY OF DIRECTIONAL AUGMENTATION CRITERIA FOR A FOUR-PROPELLERED STOL AIRPLANE

By Hervey C. Quigley, Robert C. Innis, Richard F. Vomaske, and Jack W. Ratcliff

Ames Research Center
Moffett Field, Calif.

NATIONAL AERONAUTICS AND SPACE ADMINISTRATION

For sale by the Clearinghouse for Federal Scientific and Technical Information
Springfield, Virginia 22151 – CFSTI price $3.00

A FLIGHT AND SIMULATOR STUDY OF DIRECTIONAL AUGMENTATION CRITERIA FOR A FOUR-PROPELLERED STOL AIRPLANE

By Hervey C. Quigley, Robert C. Innis, Richard F. Vomaske, and Jack W. Ratcliff

Ames Research Center

SUMMARY

A flight and simulator investigation has been conducted to determine the directional augmentation required for satisfactory lateral-directional handling qualities at low approach speeds for a large STOL airplane. The results showed that augmentation was required to reduce sideslip excursion during lateral maneuvering and to increase the directional damping.

Satisfactory directional characteristics were achieved with an augmentation system that drove the rudder in proportion to roll rate and aileron deflection to improve turn coordination and in proportion to rate change of sideslip to increase directional damping. This augmentation enabled the evaluating pilots to make acceptable hooded instrument landing approaches. The unsatisfactory lateral characteristics of the airplane prevented complete evaluation of the airplane in STOL operation.

INTRODUCTION

Several flight investigations of STOL transport airplanes (refs. 1-4) have demonstrated that good STOL performance can be obtained with the deflected slipstream principle. But the studies pointed out deficiencies in handling qualities that would limit their utilization as military assault transports or as commercial short-haul airliners. Most of the airplanes had poor lateral-directional characteristics in the landing approach and these greatly concerned the evaluating pilots.

Consequently, to study the lateral-directional control problem of large STOL airplanes, the characteristics of the NC-130B airplane were used for a simulator study; the results are reported in reference 5. The study showed that handling qualities would be satisfactory if the directional stability and sideslip rate damping were increased. To extend the simulator studies to flight, an augmentation system was incorporated in the NC-130B to drive the rudder in response to several inputs with variable gains.

The results of the investigation of the augmentation requirements for a large deflected slipstream STOL airplane are reported herein along with the pilot's evaluation of the system.

NOTATION

A_y	lateral acceleration of center of gravity as measured by an accelerometer, $\frac{1}{g}\frac{dV_e}{dt} + \frac{V}{g}r - \sin\Phi$, g units
b	wing span, ft
$C_{L_{trim}}$	trim lift coefficient
C_n	yawing-moment coefficient
C_{n_p}	$\frac{\partial C_n}{\partial(pb/2V)}$, per radian
C_{n_r}	$\frac{\partial C_n}{\partial(rb/2V)}$, per radian
C_{n_β}	$\frac{\partial C_n}{\partial\beta}$, per radian
$C_{n_{\dot\beta}}$	$\frac{\partial C_n}{\partial(\dot\beta b/2V)}$, per radian
$C_{n_{\delta_a}}$	$\frac{\partial C_n}{\partial\delta_a}$, per radian
C_y	side-force coefficient
C_{y_p}	$\frac{\partial C_y}{\partial(pb/2V)}$, per radian
C_{y_β}	$\frac{\partial C_y}{\partial\beta}$, per radian
$C_{y_{\delta_a}}$	$\frac{\partial C_y}{\partial\delta_a}$, per radian
$C_{y_{\delta_r}}$	$\frac{\partial C_y}{\partial\delta_r}$, per radian

g	acceleration of gravity, ft/sec^2
Hz	unit of frequency (1 hertz = 1 cps)
I_{xx}	moment of inertia about roll axis, slug-ft^2
I_{zz}	moment of inertia about yaw axis, slug-ft^2
m	mass, $\frac{W}{g}$, slugs
N_p	$\frac{C_{n_p} qSb^2}{2VI_{zz}}$, 1/sec
N_r	$\frac{C_{n_r} qSb^2}{2VI_{zz}}$, 1/sec
N_β	$\frac{C_{n_\beta} qSb}{I_{zz}}$, 1/sec^2
$N_{\dot{\beta}}$	$\frac{C_{n_{\dot{\beta}}} qSb^2}{2VI_{zz}}$, 1/sec
N_{δ_a}	$\frac{C_{n_{\delta_a}} qSb}{I_{zz}}$, 1/sec^2
N_{δ_r}	$\frac{C_{n_{\delta_r}} qSb}{I_{zz}}$, 1/sec^2
p	roll rate, rad/sec or deg/sec
q	free-stream dynamic pressure, lb/ft^2
r	yaw rate, rad/sec
S	wing area, ft^2
t	time, sec
V	velocity, ft/sec or knots
v_e	side velocity, ft/sec
$(v_e)_g$	side velocity due to gusts, ft/sec

W	gross weight, lb
Y_β	$\frac{C_{y_\beta} qS}{mV}$, 1/sec
Y_{δ_r}	$\frac{C_{y_{\delta_r}} qS}{mV}$, 1/sec
β	sideslip angle, degrees or radians
$\dot{\beta}$	rate change of sideslip, rad/sec
δ_a	aileron deflection, degrees or radians (Positive deflection is right aileron "up.")
δ_f	flap deflection, deg
δ_p	rudder pedal deflection, in. (Positive deflection is left pedal forward.)
δ_r	rudder deflection, degrees or radians (Positive deflection is trailing edge left.)
δ_w	lateral control wheel deflection, deg (Positive deflection is clockwise rotation.)
ρ	mass density of ambient air, slugs/ft^2
τ	time constant, sec
Φ	bank angle, radians or degrees
ψ	heading angle, deg

EQUIPMENT AND TEST

Test Airplane

A modified Lockheed C-130B (NC-130B) airplane was used for the tests. A two-view sketch of the airplane is shown in figure 1(a), and a photograph of the airplane is shown in figure 1(b). Table I presents the pertinent geometric data for the airplane.

The airplane was equipped with shroud-type, blowing boundary-layer control on the plain trailing-edge flaps, on the drooped ailerons, on the elevators, and on the enlarged rudder. The boundary-layer-control air was provided by two engines that drove load compressors mounted on outboard wing pods. The flight controls were actuated by an irreversible, fully powered, hydraulic control system. The airplane is further described in reference 2.

For this investigation the rudder control system was modified to eliminate the undesirable force characteristics noted in reference 2. The modified rudder system also included an electromechanical extendible link that was driven by the stability augmentation system.

Stability Augmentation System (SAS).- The SAS installed in the test airplane is a rudder servomechanism summed in series with the pilot's control linkage. A block diagram of the system is presented in figure 2.

Any combination of seven inputs may be summed electronically to command position of the SAS rudder servo. The servo is an electromechanical extendible link, the length of which is controlled by a motor-driven lead screw. Actually, two such servo units operate in parallel to generate the required power, and the dual combination is referred to as the SAS servo.

Each electrical input signal is provided with a gain-controlling potentiometer accessible to the crew so that individual input sensitivities can be varied in flight. The range of gains available for each input is given in table II.

The SAS servo linkage is installed in the aft fuselage, between the rudder cable bell crank and the hydraulic rudder control valve in such a manner that maximum servo travel of ±0.5 cm deflects the rudder ±15°.

This series type of mechanical summation allows forces introduced by the SAS servo to be reflected back through the control cables to the rudder pedals. These forces result from friction in the control system between the SAS servo and the rudder valve and from the forces required to actuate the valve. For this particular installation the rudder valve forces were large because of the viscous damper required on the valve actuator to insure stability of the basic, nonaugmented rudder system. Therefore, when high rates are introduced by the SAS servo, the pilot can discern objectionable force levels at the rudder pedals.

The measured frequency response of the rudder control system, driven by a constant amplitude sinusoidal signal to the SAS servo, is shown in figure 3. For this test the pedals were restrained by the feel-spring centering force. The input amplitude corresponded to approximately ±3° rudder deflection.

The response to larger amplitudes is seriously affected by rate limiting since the velocity limit of the rudder is approximately 15° per second. Also, the response to smaller amplitudes begins to become masked by the deadband. Tests indicated ±0.5° backlash in the basic rudder system. At the 3° amplitude, rate limiting enters into the response at frequencies above 0.6 Hz. However, the data can be considered valid in the range expected in flight below 0.3 Hz and the response corresponds very closely to a second order, linear system response with a damping ratio of 0.4 and a natural frequency of 0.6 Hz. In figure 3 the phase is shown to be lagging by 25° at 0.3 Hz. Again, phase shift depends on amplitude because of the effective time delay associated with backlash.

The low maximum rudder rate of 15° per second results from the high control valve forces and the limited capability of the SAS servo actuator. Tests with a more powerful servo indicated that the pilot could not tolerate higher servo rates because of the excessive force feedback to the rudder pedals.

Instrumentation.- The instrumentation was essentially the same as the equipment used in the flight tests of reference 2. Standard NASA instruments and oscillographs were used to record the following parameters:

Angular velocities about all three axes
Roll and pitch attitude
Linear acceleration at center of gravity along all three axes
Control positions of aileron, rudder, elevator, and No. 1 and No. 4 throttles
Control forces, wheel and column
Airspeed at wing tip boom
Altitude at wing tip boom
Angle of attack at wing tip boom
Angle of sideslip at wing tip boom
ILS azimuth and glide slope errors
Voltage from various SAS components

Except for the roll attitude gyro the input transducers for the SAS were separate from the recording instrumentation. The sideslip vane for the SAS was mounted on the forward portion of the fuselage above the cockpit. This vane position was calibrated by reference to the sideslip angle vane on the wing tip boom. The fuselage mounted vane had a 20-percent position error, but gave a much "clearer" signal.

Simulator

The Ames Moving Cab Transport Simulator (fig. 4) was used in conjunction with the flight test to evaluate the stability augmentation system. The simulator had limited roll and pitch motion and a projected cloud and televised runway display. Six-degree-of-freedom equation of motion for the airplane plus the kinematics of the stability augmentation system were programed on the analog computer for the simulator tests. A roll angle autopilot was included in the analog program for computing airplane response in turn entries.

Test Conditions

The NC-130B airplane in the STOL landing configuration was used to evaluate the augmentation system. In the landing configuration the flaps are deflected 70°, the ailerons are drooped 30°, and there is boundary-layer control over the flaps and control surfaces; the landing approach speed is 70 knots. The average gross weight of the test airplane was 100,000 pounds.

The flight evaluations by three NASA pilots were made from the San Jose Municipal Airport, which has a 3° approach Instrument Landing System (ILS). The pilots rated the changes in augmentation according to table III. The tasks used for the evaluation were (1) turn entries and S-turns, (2) release from sideslip and rudder pulses to excite Dutch roll, (3) VFR approaches with various offsets, (4) hooded ILS approaches, and (5) IFR operation in gusty weather.

The airplane characteristics programed on the analog computer for the computer and simulator runs were as listed in reference 5. Some minor changes were necessary to make the computed response of the airplane match the flight test data of this investigation. The evaluation tasks on the simulator were the same as those in flight.

ANALYSIS AND RESULTS

Requirements for Augmentation

In a previous flight investigation of the handling qualities of the test airplane in the STOL mode (ref. 2) a basic lateral-directional problem was found to exist at low speeds in the landing approach. The flight study and a follow-on simulation study (ref. 5) showed that low directional stability, low directional damping, and adverse yaw due to lateral control were responsible for the large sideslip excursions during maneuvers in the landing approach or during flight in gusty air at low speeds. The pilots found these sideslip excursions difficult to control and rated the airplane unacceptable (PR 7-8) for hooded IFR approaches. Whenever the pilot attempted a turn to correct a localizer error on an IFR approach, the airplane would initially tend to skid and not turn as bank angle built up. This caused a large sideslip angle and a lag of several seconds between bank angle and turn rates. With low damping and highly adverse yaw due to aileron deflection, the pilot found it almost impossible to coordinate the turn with rudder pedals. Augmentation is therefore required to improve the turn coordination.

The airplane in the STOL mode has low Dutch-roll damping ($\zeta = 0.1$). The Dutch roll was predominantly a directional oscillation with a low value of $|\Phi|/|\beta|$. The pilots found that to damp the directional oscillations, which were easily excited by either maneuvering or gusts, required considerably more time and concentration than acceptable. Augmentation is, therefore, required to increase the directional damping.

Turn coordination.- The turn coordination problem of large STOL airplanes is illustrated in figure 5. These time histories show the sideslip, yaw rate, and bank angle in a rudder-fixed turn of the test airplane at 70 knots. Because of the adverse yaw due to aileron deflection ($-N_{\delta_a}$) and adverse yaw due to roll rate ($-N_p$), the first directional response of the airplane to the abrupt aileron input is a yaw acceleration opposite to the desired turn. Sideslip immediately begins to develop because of adverse yaw and the lateral acceleration due to bank angle. Even after the ailerons are neutralized, sideslip continues to build up to a value sufficient to generate a yawing moment ($N_\beta\beta$) to turn the airplane. The simplified lateral-directional equation of motion related to turn coordination is developed in appendix A.

A convenient measure of the turn coordination of an airplane is the ratio of the peak sideslip to peak bank angle, $\Delta\beta/\Delta\Phi$, that is present in a rudder-fixed turn entry. The method used to determine $\Delta\beta$ and $\Delta\Phi$ is illustrated in figure 5. A well coordinated turn would have a low value of $\Delta\beta/\Delta\Phi$ (i.e., very little sideslip in a turn). The variation of $\Delta\beta/\Delta\Phi$ with airspeed between 65 and 120 knots for the test airplane is shown in figure 6. The data show that $\Delta\beta/\Delta\Phi$ increases as airspeed is reduced; at airspeeds less than 100 knots, $\Delta\beta/\Delta\Phi$ is greater than 0.3 and turn coordination becomes poor.

There are four terms in the equations of motion of an airplane in flight that can account for the increase in $\Delta\beta/\Delta\Phi$ as airspeed is reduced: (1) an increase in turn rate for a given bank angle ($r \approx (g/V)\Phi$), (2) a decrease in directional stability, N_β, (3) an increase in adverse yaw due to aileron deflection, $-N_{\delta_a}$, and (4) an increase in adverse yaw due to roll rate, $-N_p$. All are evident in the test airplane. The simulator study of reference 5 showed that turn entry characteristics are improved substantially at low airspeed when the directional stability is increased. Further analysis (appendix A) shows, however, that for perfectly coordinated turns (zero β), directional stability N_β is not required, but the yaw due to roll rate must be the proper positive value ($N_p = g/V$). This investigation was, therefore, centered on the use of yaw due to roll rate for turn augmentation.

The yawing moments required to coordinate a turn must be developed by rudder deflection. Appendix A shows that for a zero sideslip turn, rudder deflection must produce yawing moments proportional to roll rate, $\delta_r/p = -(N_p - g/V)/N_{\delta_r}$, to aileron deflection (to correct for adverse yaw $\delta_r/\delta_a = -N_{\delta_a}/N_{\delta_r}$), and to yaw rate (to compensate for the inherent yaw rate damping of the airplane, $\delta_r/r = -N_r/N_{\delta_r}$). The relative magnitude and phasing of these three inputs are illustrated in figure 7. The figure shows an analog-computed time history of a typical coordinated 10° bank turn in which the required rudder deflection due to roll rate, yaw rate, and aileron deflection has been separated incrementally. Large increments of rudder deflection due to roll rate and aileron deflection are evident for this relatively mild turn. The incremental rudder deflection due to yaw rate is small but in phase with the yaw rate driving the directional damping to zero. Fortunately, since the amount of sideslip resulting from turn rate is small and easy for the pilot to control, the δ_r/r term need not be included in the turn coordination augmenter.

Yaw rate damping.- The second requirement for augmentation is satisfactory directional damping. The basic damping of the test airplane is low with a damping ratio of only 0.1 ($t_{1/2}$ = 15 sec). The simulator test of reference 5 indicated little gain in pilot rating with yaw rate damping unless the stability was also increased. Since yaw dampers have been successfully used on many conventional airplanes, further study was made to determine if yaw dampers are suitable for STOL airplanes. The analysis showed that an increase in the steady-state sideslip in a rudder-fixed turn accompanies increases in yaw rate damping. This is illustrated in figure 8 which shows how the ratio of steady-state sideslip angle to steady-state bank angle, β/Φ, varies with yaw rate damping (N_r). These data show that for a satisfactory level of damping

(N_r = -0.4 to -0.6), a sideslip angle of about one-half the bank angle (β/Φ = 0.5) will develop in a steady-state turn. The yaw damper tends to introduce more undesirable sideslip. A "washout" in the yaw damper circuit would reduce the sideslip in a steady turn, but such a circuit would have little effect on the peak value of $\Delta\beta/\Delta\Phi$.

Since steady-state β/Φ for yaw rate dampers is inversely proportional to airspeed as shown by the equation on figure 8, yaw rate dampers are satisfactory at high airspeeds, but are unsatisfactory at the low approach speeds of STOL airplanes.

Sideslip rate damping.- Sideslip rate damping (referred to as $\dot{\beta}$ damping) was not found to have the difficulties of yaw rate damping discussed in the preceding section. Figure 9 illustrates the differences by comparing time histories of turn entries with the two types of damping. With $\dot{\beta}$ damping the peak sideslip is lower as is the sideslip in the steady-state portion of the turn. In releases from sideslip or rudder step maneuvers the differences are small. The results of the simulator studies of the test airplane (ref. 5) and the flight tests with the BLC equipped Boeing 367-80 (ref. 6) as well as the flight studies of this investigation have confirmed the superiority and effectiveness of $\dot{\beta}$ damping.

Although $\dot{\beta}$ damping is desirable, problems have arisen in mechanization. Since there is no known way to achieve $\dot{\beta}$ damping aerodynamically, augmentation schemes had to be developed. A method used in this study and in reference 6 was to differentiate the signal from a sideslip vane. This proved quite successful in calm air, but unsatisfactory in gusty air or turbulence where, of course, good damping characteristics are needed. The problem was that the system responded to the rate change of side gust velocity instead of attempting to damp the response of the airplane to the gust. The solution, therefore, was to produce a $\dot{\beta}$ input signal that was a function of the rate change of the flight path of the airplane instead of the free air. The method and equation used for deriving such a signal are developed and discussed in appendix B. In figure 10 the two types of $\dot{\beta}$ damping are compared for an airplane flying through mild turbulence. With a vane input, large amplitude rudder motions forced the airplane into undesirable yawing motions that were quite objectionable to the pilot both from a comfort and control standpoint. With airplane response inputs the rudder input is small and is proportional to the amount of the gust that is disturbing the airplane.

After flying with various amounts of damping, the pilot selected a level that gave only a small overshoot (damping ratio between 0.4 and 0.5) in sideslip or yaw rate with rudder steps or releases from sideslip. More damping was good in rough air and sidestep maneuvers, but made the airplane too sluggish in decrabbing maneuvers. Less damping required too much pilot effort.

Augmentation Techniques

The methods and techniques used in the augmentation of the lateral-directional characteristics of the test airplane to improve its handling

qualities will be discussed in this section. The stability augmentation system (SAS) that was used to drive the rudder in response to various inputs is described in the Equipment and Test section of the report.

SAS inputs.- The SAS system had multiple inputs all with variable gains and therefore many combinations of inputs were available. Much of the test flying of the airplane was devoted to determining a satisfactory configuration within the limits of the SAS. An SAS configuration was chosen on the basis of the requirements discussed in the preceding section. The following table lists the inputs and gains used:

Input	Purpose	Gain	Estimated augmented derivative
δ_a	Reduce adverse yaw	$\delta_r/\delta_a = -0.24$	$N_{\delta_a} = 0$
p	Turn coordination	$\delta_r/p = -1.3$ sec	$N_p = 0.23$
Φ r A_y	Directional damping	$\delta_r/\Phi = -0.4$ $\delta_r/r = 1.5$ sec $\delta_r/A_y = -0.4$ rad/g	$N_{\dot{\beta}_p} = 0.27$

The aileron input gain was the value estimated to give near zero yawing moment with full control. It was found, however, that the yawing moment due to aileron deflection was not linear. The gain listed in the table was too high for small wheel inputs required, and was noticeable to the pilot when he was compensating for the spiral instability in a steady turn; the pilots preferred the gain listed because of the better turn entry characteristics. The roll rate (p) input gain was set to give the augmented airplane an N_p of about g/V at the approach speed of 70 knots. The value used in the evaluation was estimated from flight test data to be 0.23 (i.e., 0.85 g/V). At airspeeds much above 100 knots in the climb after take-off or in the transition to approach speeds, the augmented N_p was too high and disturbing to the pilot. It was necessary, therefore, not to engage the SAS at too high an airspeed during transition and to disengage the system soon after take-off. This aspect posed a problem for N_p augmentation but could be solved by either introducing a velocity term into the gain computations or simply cutting the N_p input in and out as a function of airspeed or perhaps flap deflection.

The $\dot{\beta}_p$ damper inputs, which consisted of a summation of roll angle, Φ, yaw rate, r, and lateral acceleration, A_y, gains, were set to give a damping ratio of about 0.4. The optimum gains for the Φ and A_y inputs to the $\dot{\beta}$ damper vary with speed while the r input does not. The $\dot{\beta}_p$ damper can only be optimized for one airspeed. The gains listed were satisfactory for speeds between about 60-90 knots.

Simulation of SAS.- It was found early in the program that the 15° per second maximum rudder rate with the augmentation servo and the 15° rudder deflection authority of the SAS caused large lags and nonlinearities between input signals and rudder deflection. To study the effects of these lags and nonlinearities the test airplane characteristics and the SAS characteristics were programed on the analog computer. Both analog computer runs and a piloted simulation were conducted to compare the lateral-directional characteristics of the simulated airplane with various rates and authorities in the SAS.

Figure 11 is a block diagram of the SAS, as simulated on the analog computer. The program included a simple lateral axis autopilot that would give a bank angle response of 10°, 20°, or 30° which was similar to piloted flight. In figure 12 the computer response is compared with actual flight. Good agreement in control deflections, bank angle, and turn rate is indicated for a 20° bank turn. The response of the simulated airplane with various SAS characteristics was then compared and the results for four different SAS characteristics are presented in table IV. The no SAS case is also shown for comparison. The peak sideslip angle shows the effectiveness of the SAS in achieving turn coordination. Peak adverse yaw rate is a measure of the effectiveness of the SAS to compensate for the adverse yaw due to aileron and roll rate. Configuration No. 2 is the simulated SAS in the airplane, No. 3 is the same system with increased servo actuator rate, and No. 4 is a nearly ideal system with the rate and authority equal to the capability of the basic aircraft rudder system. The table shows that all the systems perform a relatively good 10° bank turn entry ($\beta < 3^{\circ}$, $r < 0.01$) but require almost all of the SAS servo authority (i.e., 14.5° vs 15° rudder deflection). For 30° bank turns a maximum servo rate of at least 30° per second and rudder authority of about 40° would be required.

The pilot, performing a lateral offset task on the simulator, could tell little difference between the various SAS characteristics except in maneuvers that required more than 15° of bank.

The effect of the lags on damping was small unless the rudder deflection was at the augmentation servo limit. With the SAS of the test airplane simulated (configuration No. 2 on table IV), the pilot disliked the sudden change in damping characteristics in large bank angle maneuvers where the rudder deflections required would be greater than the maximum available. The lags had some small effects on the directional frequency at large amplitude in sideslip, but not enough to be noticeable to the pilot.

Although peak sideslip and peak turn rate in the simulated turn maneuver were similar for several different SAS configurations, the phase was different as illustrated in figure 13. The first peak value of sideslip, for example, occurs at about 2-1/2 seconds of the maneuver for configuration No. 4 while the same value of β occurs at about 7 seconds for configuration No. 5. On the simulator, the differences shown were barely noticeable to the pilot. They do, however, compromise the data analysis for defining the effect of parameter changes on the airplane lateral-directional characteristics.

From the results of the analog computer and simulator study it was concluded that the pilot opinion data obtained in flight with the test airplane

would be valid for offset maneuvers where bank angles between 15° and 20° are normally used. The flight data will show the inputs required and the effectiveness of directional augmentation in improving the handling qualities of STOL airplanes.

Pilot Flight Evaluation

A pilot's evaluation was conducted to assess the effect of the SAS on the pilot opinion of the lateral-directional handling qualities of the test airplane at 70 knots airspeed. Early in the evaluation program it became apparent that the lateral control characteristics were unsatisfactory (pilot rating, 6-1/2), and that they made it difficult to evaluate the augmented turn coordination and directional damping characteristics. The unsatisfactory characteristics were the low lateral control power and sensitivity, poor lateral control centering and high friction, and spiral instability. To evaluate the effects of the SAS on the handling qualities, the pilot first performed the evaluating maneuver without SAS and then with SAS. In this manner he was able to separate, to some degree, the effects of SAS from the unsatisfactory lateral characteristics. The pilot ratings for the two characteristics were:

	SAS off	SAS on
Turn coordination	7-8	3-1/2
Directional damping	6-1/2	3-1/2

Obviously, augmentation was effective in providing the pilot with satisfactory turn coordination and damping characteristics. The pilot also noted significant improvements in the hooded ILS task. Without augmentation they found it impossible (pilot rating 7-8) to make ILS approaches because of the difficulty in tracking the localizer beam. The problem was due to a combination of effects which saturated the pilot's ability to cope with all of the control requirements. VFR approaches were possible, however, because precise heading control was not required. With SAS, successful ILS approaches were possible even in mild turbulence. The SAS also greatly reduced the pilot's workload by eliminating the need for him to constantly correct sideslip excursions and to damp the yawing oscillations.

Although the pilots rated turn coordination and directional damping 3-1/2 in ILS approaches, their overall lateral-directional rating was 6-1/2 because of the poor lateral control characteristics.

In the approach the limitations of the SAS, discussed in the preceding section, were not apparent to the pilot because of the small peak bank angle and low roll rates required in the approaches used. Figure 14 shows the variation of altitude and offset distance to perform a sidestep maneuver assuming a sinusoidal banking angle variation with time for peak bank angles of 10° and 20°, and, separately, roll rates of 5° and 10° per second. These data were

computed by the method of reference 7 and correlate well with flight data. The data show that at these low airspeeds and at a flight-path angle of -5°, less than 150 feet of altitude is required to perform a 300-foot lateral offset with a maximum bank angle of 20° and a maximum roll rate of 10° per second. The pilots felt, however, that the capability to make a precision turn with bank angles as high as 30° would be desirable in STOL airplanes where airspace patterns are minimum.

Even with augmentation, the pilots considered the handling qualities of the airplane to be deficient for low speed approaches. The pilots' comments indicated that several improvements would be required before the airplane could be completely evaluated in STOL operations. The SAS system would have to be improved by increasing the actuator rates and the maximum rudder authority to permit maneuvering to higher bank angles and higher roll rates.

The mechanical characteristics of the lateral control system should be improved by reducing the friction and providing positive centering. The wheel deflection for maximum rolling moment should be reduced to increase the lateral control sensitivity; this change would also require an increase in the maximum actuation rate of the aileron to prevent the pilot from experiencing nonlinear force characteristics. And, perhaps most important, lateral augmentation should be provided to stabilize the spiral mode.

SUMMARY OF RESULTS

This flight and simulator study investigated techniques for augmenting the lateral-directional characteristics of a large STOL transport airplanes to improve handling qualities in the landing approach.

For the airplane tested, augmentation was required to help the pilot control sideslip when maneuvering in the approach or when making approaches in gusty weather. With augmentation to improve the turn coordination and directional damping, the sideslip excursions could be reduced satisfactorily.

Turn coordination was augmented with a system that drove the rudder in proportion to roll rate and aileron deflection. For satisfactory turn coordination the system did not eliminate all sideslip, but the peak sideslip to peak bank angle ratio was reduced to less than 0.3 in a rudder-pedal-fixed turn entry.

Directional damping was augmented with a system that drove the rudder in proportion to the rate change of sideslip relative to the airplane flight path. This damper system derived its inputs from internally mounted instruments (roll attitude, yaw rate, and lateral acceleration) and, therefore, excluded the random inputs due to sharp edged gusts. The gain of the sideslip rate damper was adjusted to give a damping ratio of between 0.4 and 0.5.

The rudder authority for augmentation depends on the maneuvering required of the airplane in the landing approach. For the NC-130B airplane of this

investigation 25-percent rudder authority (15°) enabled the airplane to be maneuvered to a bank angle of about 15° at the 70-knot landing approach speed. Higher maneuvering capability and, therefore, higher rudder authority will be demanded for most STOL missions.

Ames Research Center
National Aeronautics and Space Administration
Moffett Field, Calif., 94035, Sept. 7, 1966
721-04-00-02-00-21

APPENDIX A

RUDDER REQUIRED FOR TURN ENTRIES

The rigorous solution to the turn entry problem is best solved on an analog or digital computer. The rudder required for turn entries can be approximated, however, by the following simplified equations and assumptions. The simplified solution is presented to show the more important terms that must be considered in a stability augmentation system for STOL airplanes. Results of both rigorous computer analysis and actual flight-test results with stability augmentation systems indicate this simplified approach to be satisfactory for analysis of airplane handling qualities.

The simplified lateral-directional equations of motion used in the derivation are as follows:

$$C_{L_{trim}}\Phi + C_{y_\beta}\beta + C_{y_{\delta_r}}\delta_r + C_{y_p}\frac{pb}{2V} + C_{y_{\delta_a}}\delta_a = \frac{2m}{\rho SV}\left(\frac{d\beta}{dt} + r\right) \tag{A1}$$

$$C_{n_\beta}\beta + C_{n_p}\frac{pb}{2V} + C_{n_r}\frac{rb}{2V} + C_{n_{\delta_a}}\delta_a + C_{n_{\delta_r}}\delta_r = \frac{2}{\rho SbV^2} I_{zz}\frac{dr}{dt} \tag{A2}$$

Letting

$$C_{y_{\delta_r}}\delta_r = C_{y_{\delta_a}}\delta_a = C_{y_p}\frac{pb}{2V} = 0$$

equation (A1) in dimensional coefficients becomes

$$\frac{d\beta}{dt} = \frac{g}{V}\Phi - r + Y_\beta\beta \tag{A3}$$

and equation (A2) in dimensional coefficients becomes

$$\frac{dr}{dt} = N_\beta\beta + N_p p + N_r r + N_{\delta_a}\delta_a + N_{\delta_r}\delta_r \tag{A4}$$

To maintain zero sideslip in a turn entry

$$\frac{d\beta}{dt} = 0$$

$$\beta = 0$$

Equation (A3) reduces to

$$\left.\begin{aligned} 0 &= \frac{g}{V}\Phi - r + 0 \\ r &= \frac{g}{V}\Phi \end{aligned}\right\} \tag{A5}$$

and differentiation of equation (A5) gives

$$\frac{dr}{dt} = \frac{g}{V} p \tag{A6}$$

Solving equations (A4) and (A6) simultaneously for δ_r in terms of Φ, r, and δ_a

$$\delta_r = \left[\frac{(g/V) - N_p}{N_{\delta_r}}\right] p - \frac{N_r}{N_{\delta_r}} r - \frac{N_{\delta_a}}{N_{\delta_r}} \delta_a \tag{A7}$$

Since the δ_a term is for correcting adverse yaw due to aileron deflection, and the r term for compensating for yawing moment due to turn rate, the terms remaining are those required for turn coordination. The requirement for zero sideslip turn entries is

$$\delta_r = -\left[\frac{N_p - (g/V)}{N_{\delta_r}}\right] p \tag{A8}$$

or

$$N_p = g/V \tag{A9}$$

APPENDIX B

DEVELOPMENT OF EQUATIONS FOR SIDESLIP RATE DAMPERS

The development of the equations used in the design of sideslip rate dampers is based on the same simplified lateral equation of motion used in appendix A. It was assumed that there were no aerodynamic $\dot{\beta}$ derivatives and that the angles were so small that the sine of the angle was equal to the angle in radians and that the cosine of the angle was equal to one.

$$C_{L_{trim}}\Phi + C_{y_\beta}\beta + C_{y_{\delta_r}}\delta_r + C_{y_p}\frac{pb}{2V} + C_{y_{\delta_a}}\delta_a = \frac{2m}{\rho SV}\left(\frac{d\beta}{dt} + r\right) \tag{B1}$$

If

$$A_y = \frac{qS}{mg}\left[C_{y_\beta}\beta + C_{y_{\delta_r}}\delta_r + C_{y_p}\frac{pb}{2V} + C_{y_{\delta_a}}\delta_a\right]$$

and

$$C_{L_{trim}} = \frac{W/S}{q} = \frac{gm}{qS}$$

equation (B1) becomes

$$\frac{d\beta}{dt} = \frac{g}{V}\Phi - r + \frac{g}{V}A_y \tag{B2}$$

In this expression $d\beta/dt$ is defined as the rate change of the difference between the flight-path angle in the horizontal plane and the airplane heading and will be referred to as $\dot{\beta}_p$.

$$\dot{\beta}_p = \frac{g}{V}\Phi - r + \frac{g}{V}A_y \tag{B3}$$

The rate change of sideslip that would be measured by a sideslip vane, $\dot{\beta}_V$, is the rate change of the angle between the free air stream and the airplane axis. Measured in this manner, $\dot{\beta}_V$ would include gusts.

$$\dot{\beta}_V = \frac{g}{V}\Phi - r + \frac{g}{V}A_y + \frac{(\dot{v}_e)_g}{V} \tag{B4}$$

where $(\dot{v}_e)_g$ is the rate change of side velocity due to gusts.

VANE-TYPE $\dot{\beta}$ DAMPER

For a vane type of $\dot{\beta}$ damper the input to the augmentation can be obtained from a vane that senses sideslip angle. The equation for the damper includes a differentiating term and a filter term as follows:

$$N_{\dot{\beta}_V} = N_{\delta_r} \frac{\delta_r}{\dot{\beta}_V} \tag{B5}$$

where

$$\dot{\beta}_V = \frac{\beta s}{(\tau_1 s + 1)(\tau_2 s + 1)} \tag{B6}$$

τ_1 time constant in differentiation

τ_2 time constant in filter

s Laplace operator

For the test airplane the following values were used:

$$\tau_1 = 0.02 \text{ sec}$$

$$\tau_2 = 0.4 \text{ sec}$$

PATH-TYPE $\dot{\beta}$ DAMPER

For the path-type $\dot{\beta}$ damper the input to the augmentation is obtained from internally mounted instruments.

Equation (B3) shows that at a constant velocity the three inputs required are Φ, r, and A_y. The input Φ can be measured with an attitude gyro; r, with a rate gyro; and A_y, with a lateral accelerometer at the center of gravity of the airplane. With these inputs the equation for the $\dot{\beta}_p$ damper is as follows.

$$N_{\dot{\beta}_p} = N_{\delta_r} \frac{\delta_r}{\dot{\beta}_p} \tag{B7}$$

Expanding by use of the expression in equation (B3) for $\dot{\beta}_p$

$$N_{\dot{\beta}_p} = \frac{V}{g} N_{\delta_r} \frac{\delta_r}{\Phi} - N_{\delta_r} \frac{\delta_r}{r} + \frac{V}{g} N_{\delta_r} \frac{\delta_r}{A_y} \tag{B8}$$

and the ratios of rudder deflection to the inputs Φ, r, and A_y are

$$\frac{\delta_r}{\Phi} = \frac{g}{V} \frac{N_{\dot{\beta}_p}}{N_{\delta_r}}$$

$$\frac{\delta_r}{r} = - \frac{N_{\dot{\beta}_p}}{N_{\delta_r}}$$

$$\frac{\delta_r}{A_y} = \frac{g}{V} \frac{N_{\dot{\beta}_p}}{N_{\delta_r}}$$

For the test airplane at a satisfactory level of damping at 70-knots approach speed the following values were used:

$$N_{\dot{\beta}_p} = 0.3 \text{ 1/sec}$$

$$\frac{\delta_r}{\Phi} = -0.4 \text{ rad/rad}$$

$$\frac{\delta_r}{r} = 1.5 \text{ rad/rad/sec}$$

$$\frac{\delta_r}{A_y} = -0.4 \text{ rad/g}$$

SIMPLIFIED PATH-TYPE $\dot{\beta}$ DAMPER

For STOL airplanes the δ_r/A_y term contributes very little to the damping because of the low aerodynamic side forces at low airspeed. Experience with the test airplane has shown that omitting this term from the damper has little effect on either pilot opinion or damping ratio. If δ_r/A_y is omitted, the $\dot{\beta}_p$ damper equation becomes:

$$N_{\dot{\beta}_p} = \frac{V}{g} N_{\delta_r} \frac{\delta_r}{\Phi} - N_{\delta_r} \frac{\delta_r}{r} \tag{B9}$$

and the ratios of rudder deflection to the inputs Φ and r are

$$\frac{\delta_r}{\Phi} = \frac{g}{V} \frac{N_{\dot{\beta}_p}}{N_{\delta_r}}$$

$$\frac{\delta_r}{r} = - \frac{N_{\dot{\beta}_p}}{N_{\delta_r}}$$

REFERENCES

1. Innis, Robert C.; and Quigley, Hervey C.: A Flight Examination of Operating Problems of V/STOL Aircraft in STOL-Type Landing and Approach. NASA TN D-862, 1961.

2. Quigley, Hervey C.; and Innis, Robert C.: Handling Qualities and Operational Problems of a Large Four-Propeller STOL Transport Airplane. NASA TN D-1647, 1963.

3. Quigley, Hervey C.; Innis, Robert C.; and Holzhauser, Curt A.: A Flight Investigation of the Performance, Handling Qualities, and Operational Characteristics of a Deflected Slipstream STOL Transport Airplane Having Four Interconnected Propellers. NASA TN D-2231, 1964.

4. Holzhauser, Curt A.; Innis, Robert C.; and Vomaske, Richard F.: A Flight and Simulator Study of the Handling Qualities of a Deflected Slipstream STOL Seaplane Having Four Propellers and Boundary-Layer Control. NASA TN D-2966, 1965.

5. Quigley, Hervey C.; and Lawson, Herbert F., Jr.: Simulator Study of the Lateral-Directional Handling Qualities of a Large Four-Propellered STOL Transport Airplane. NASA TN D-1773, 1963.

6. Gratzer, L. B.; and O'Donnell, T. J.: Development of a BLC High-Lift System for High-Speed Airplanes. J. Aircraft, vol. 2, Nov.-Dec. 1965, pp. 477-484. (AIAA paper 64-589.)

7. Perry, D. H.; Port, W. G. A.; Morrell, J. C.: A Flight Study of the Sidestep Manoeuvre During Landing. R & M 3347, British ARC, 1964.

TABLE I.- GEOMETRIC DATA

Wing	
Total area, sq ft	1745.5
Span, ft	132.69
Mean aerodynamic chord, ft	13.71
Taper ratio	.52
Aspect ratio	10.09
Angle of incidence, deg	
Root	0
Tip	-3.0
Airfoil section	
Root	NACA 64A318
Tip	NACA 64A412
Dihedral (lower surface), deg	2.3
Flap	
Area, sq ft	287.8
Span (each side), ft	
Inboard	11.3
Outboard	26.2
Deflection (maximum), deg	90.0
Chord (percent wing chord)	25.0
Aileron	
Area, sq ft	110.0
Span (each side)	18.8
Chord (percent wing chord)	28.0
Droop, deg	30.0
Travel (maximum from wing-chord line)	
Normal, deg	
Up	30.0
Down	19.0
Drooped, deg	
Up	30.0
Down	60.0
Horizontal tail	
Area, sq ft	543.0
Span, ft	52.7
Airfoil section	NACA 23012
Elevator area, sq ft	154.0
Elevator travel (maximum), deg	
Up	49.0
Down	38.5
Vertical tail	
Area, sq ft	330.0
Span, ft	23.1
Airfoil section	Modified NACA 64A016
Rudder area, sq ft	98.6
Rudder travel (maximum), deg	±60.0

TABLE II.- SAS INPUTS AND GAINS

Input parameter	Range of gains
β	$\frac{\delta_r}{\beta}$ = 0 to ±6 rad/rad
$\dot{\beta}$	$\frac{\delta_r}{\dot{\beta}}$ = 0 to -2.3 rad/rad/sec
p	$\frac{\delta_r}{p}$ = 0 to -3 rad/rad/sec
Φ	$\frac{\delta_r}{\Phi}$ = 0 to -0.6 rad/rad
r	$\frac{\delta_r}{r}$ = 0 to 3 rad/rad/sec
A_y	$\frac{\delta_r}{A_y}$ = 0 to -1.7 rad/g
δ_a	$\frac{\delta_r}{\delta_a}$ = 0 to -0.45 rad/rad

TABLE III.- PILOT OPINION RATING SYSTEM

	Adjective rating	Numerical rating	Description	Primary mission accomplished	Can be landed
Normal operation	Satisfactory	1	Excellent, includes optimum	Yes	Yes
		2	Good, pleasant to fly	Yes	Yes
		3	Satisfactory, but with some mildly unpleasant characteristics	Yes	Yes
Emergency operation	Unsatisfactory	4	Acceptable, but with unpleasant characteristics	Yes	Yes
		5	Unacceptable for normal operation	Doubtful	Yes
		6	Acceptable for emergency condition only[a]	Doubtful	Yes
No operation	Unacceptable	7	Unacceptable even for emergency condition[a]	No	Doubtful
		8	Unacceptable - dangerous	No	No
		9	Unacceptable - uncontrollable	No	No

[a]Failure of a stability augmenter.

TABLE IV.- RESULTS OF SAS SIMULATION

SAS configuration				β peaks		Peak adverse yaw rate		Peak rudder deflection	
No.	System[a]	Max. servo rate	Max. servo authority	$\Phi = 10^\circ$	$\Phi = 30^\circ$	$\Phi = 10^\circ$	$\Phi = 30^\circ$	$\Phi = 10^\circ$	$\Phi = 30^\circ$
1	---	---	---	7.2	> 15	0.02	0.06	0	0
2	A	15	15	2.4	10.4	.01	.04	14.5	15 (limit)
3	A	30	15	2.0	9.6	.004	.032	14.5	15 (limit)
4	A	30	60	2.0	5.5	.004	.01	14.5	34.0
5	B	60	60	1.9	5.2	.004	.01	13	40

[a]System A. $$\delta_r = \frac{1.4p + 0.3\delta_a + 1.5\dot{\beta}}{(0.1s + 1)[(s^2/16) + (3.2s/16) + 1]}$$

B. $$\delta_r = \frac{1.4p + 0.3\delta_a + 1.5\dot{\beta}}{(0.1s + 1)}$$

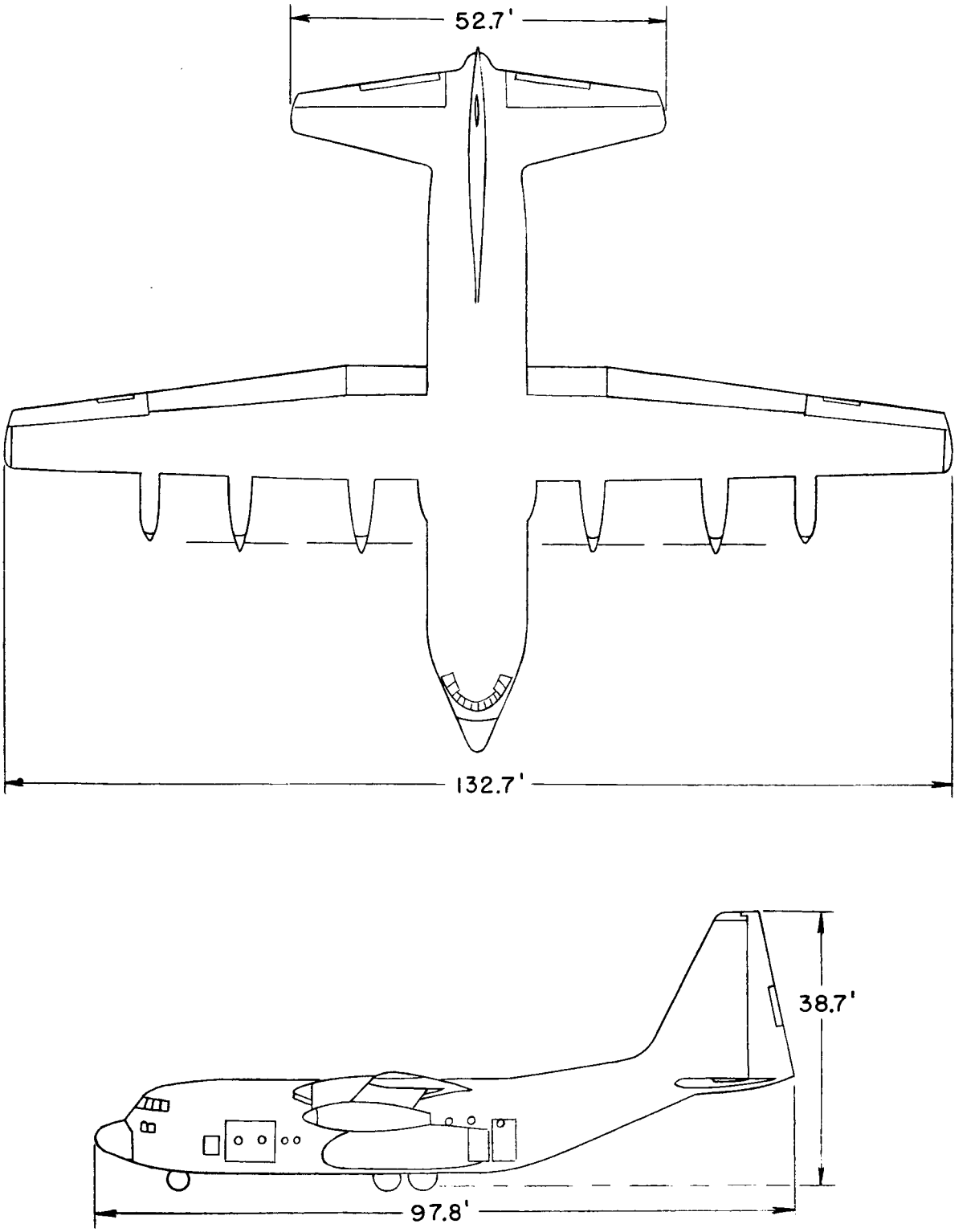

(a) Sketch of test airplane.

Figure 1.- A modified Lockheed C-130B (NC-130B) airplane.

A-28387

(b) Test airplane.

Figure 1.- Concluded.

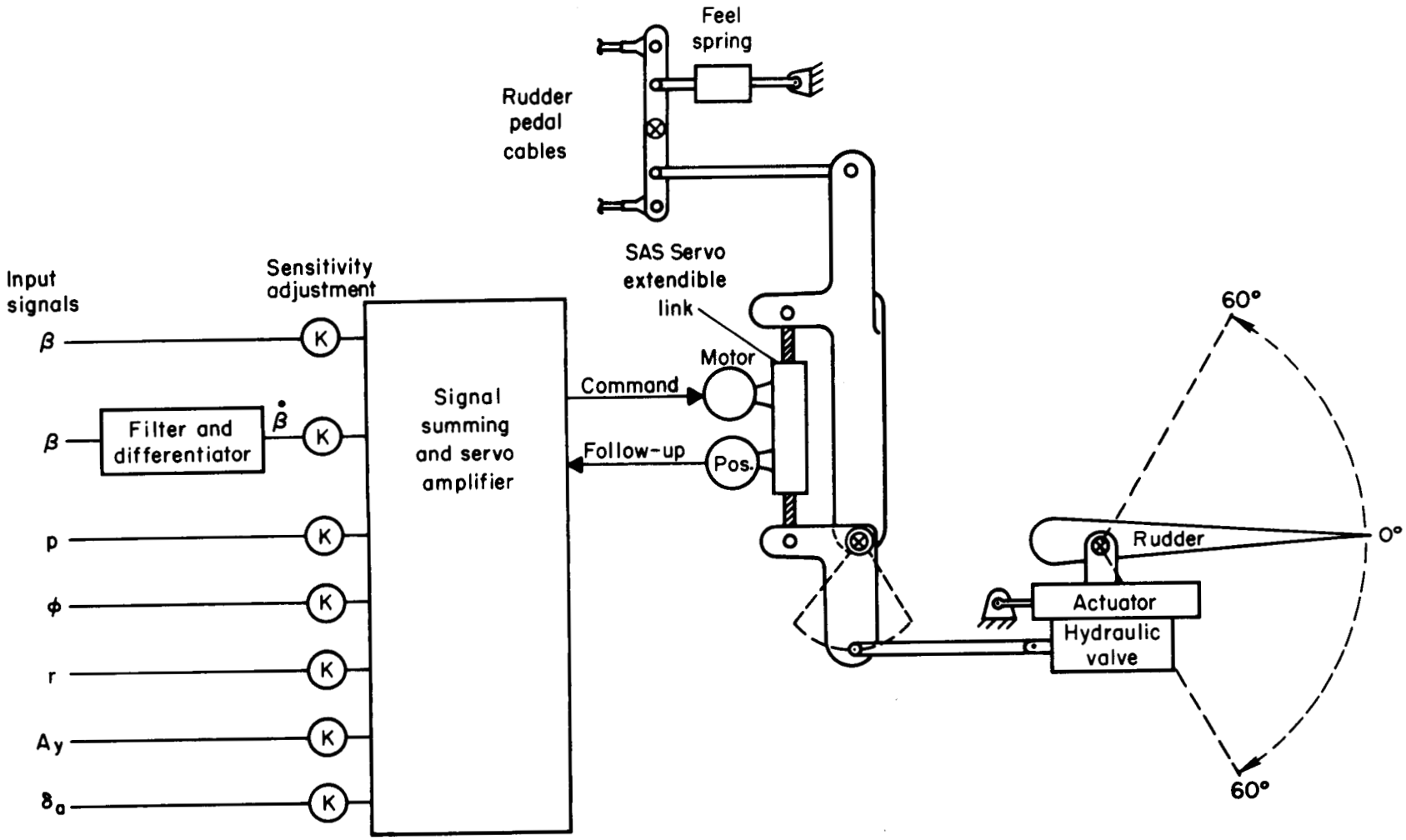

Figure 2.- Block diagram of SAS.

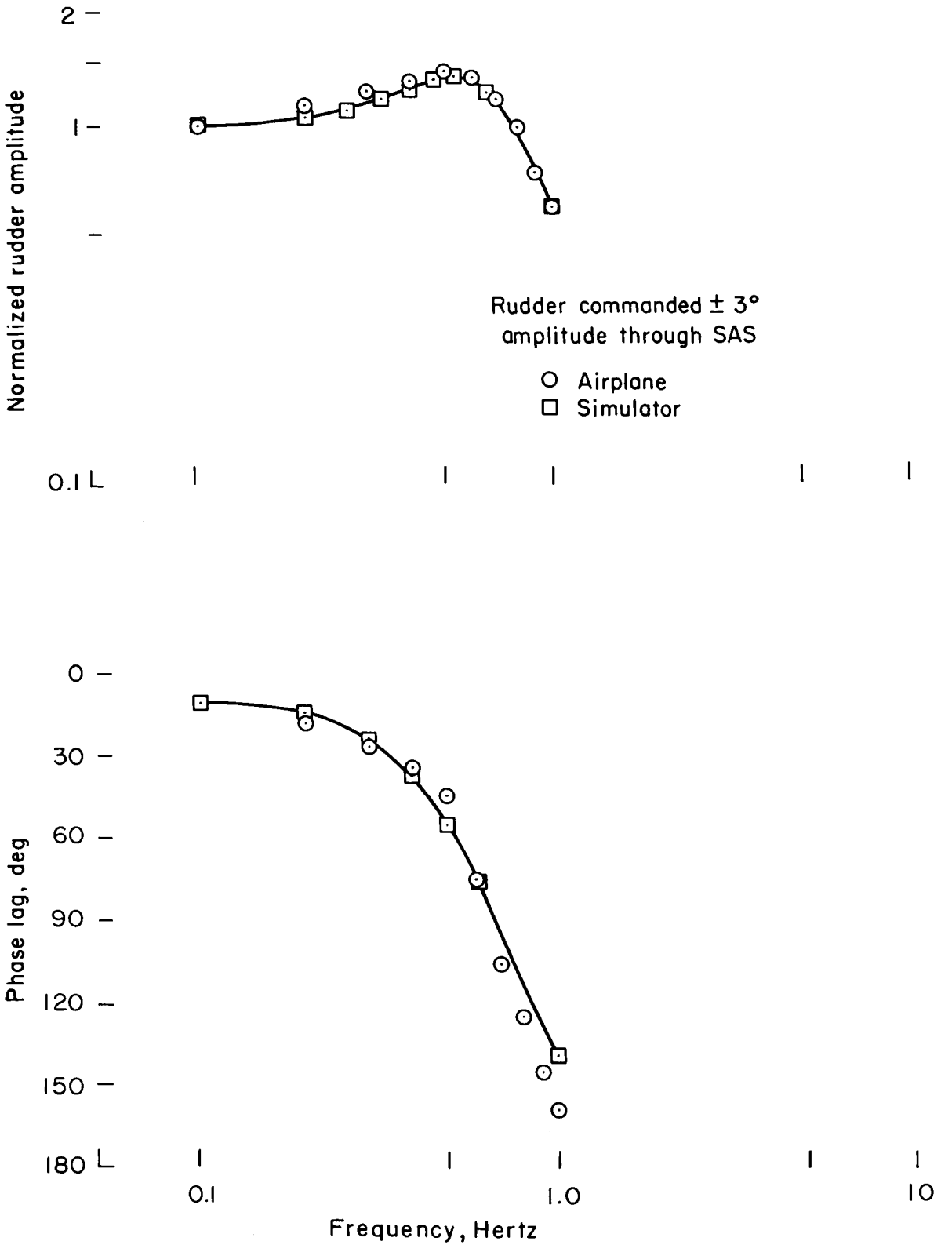

Figure 3.- Rudder frequency response.

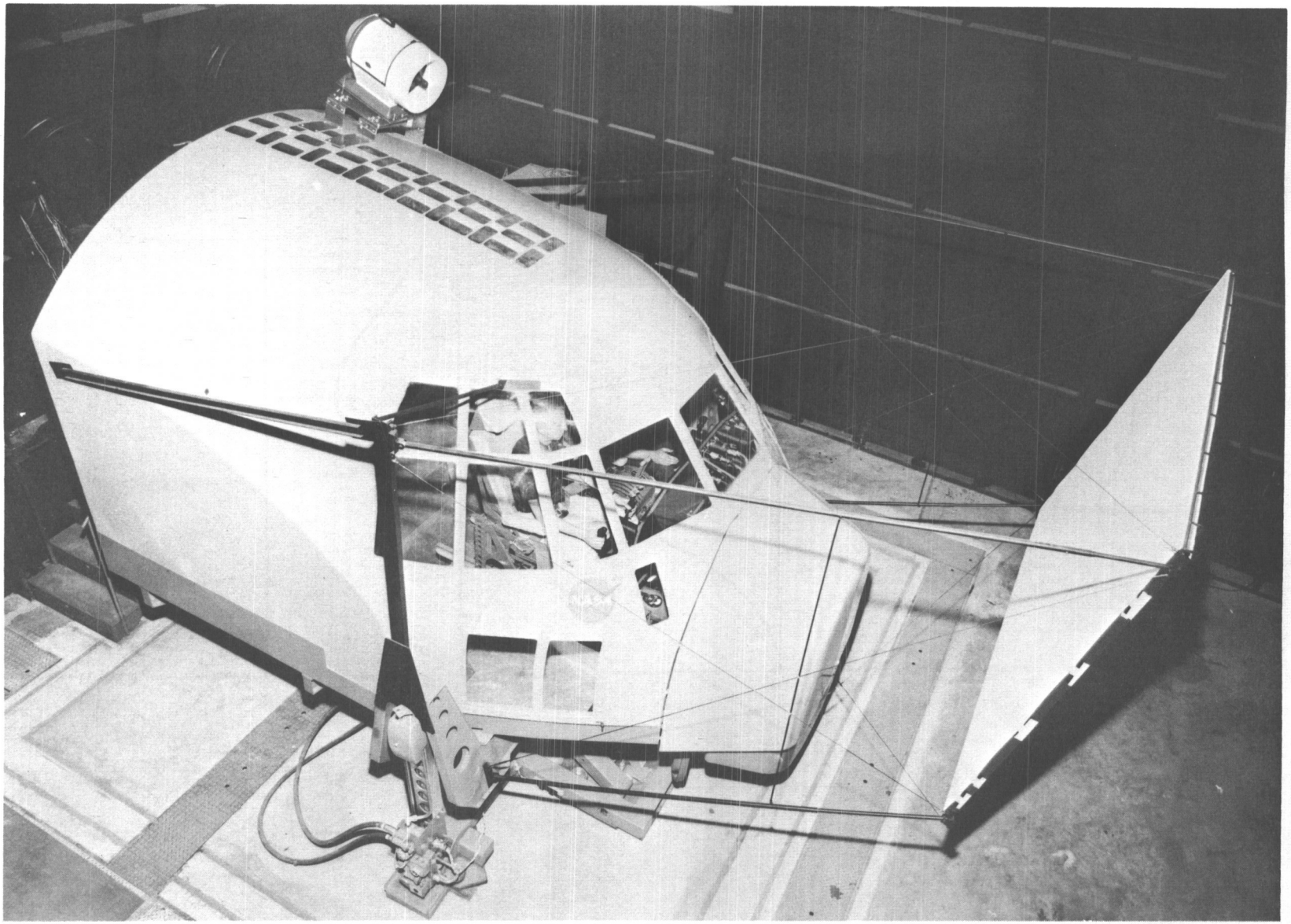

A-30526-15

Figure 4.- Ames Moving Cab Transport Simulator.

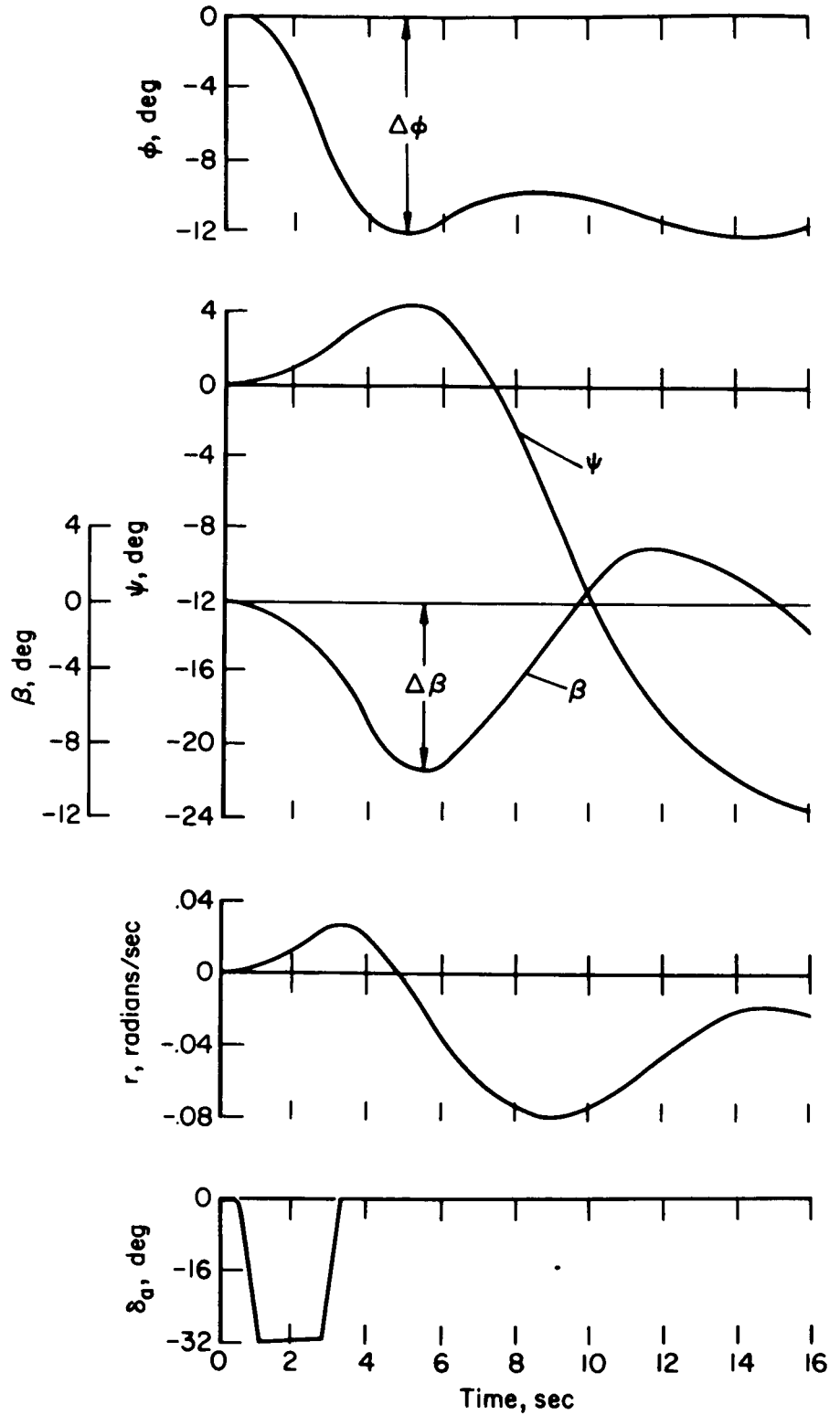

Figure 5.- Time history of the response to a lateral control input; V ≈ 70 knots.

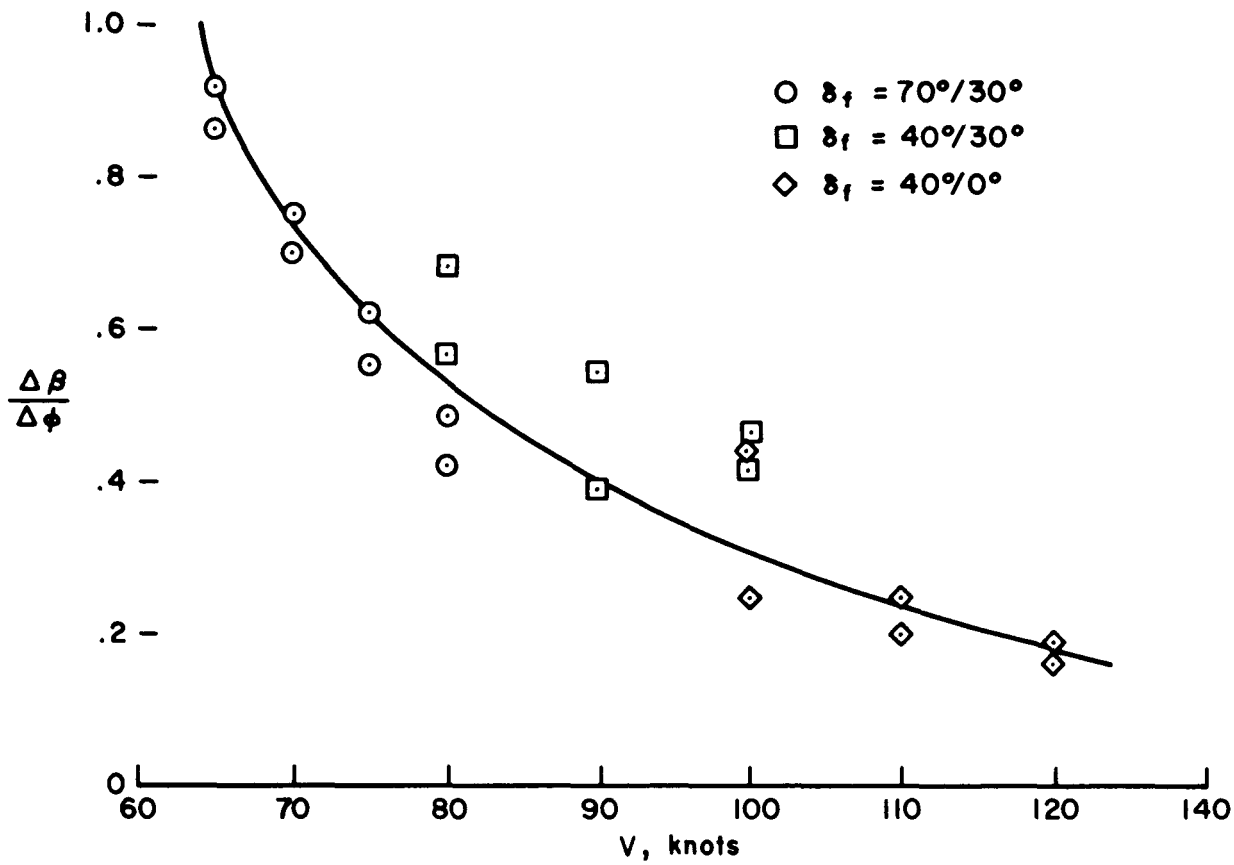

Figure 6.- Variation of the turn coordination parameter ($\Delta\beta/\Delta\Phi$) with airspeed for test airplane; SAS off.

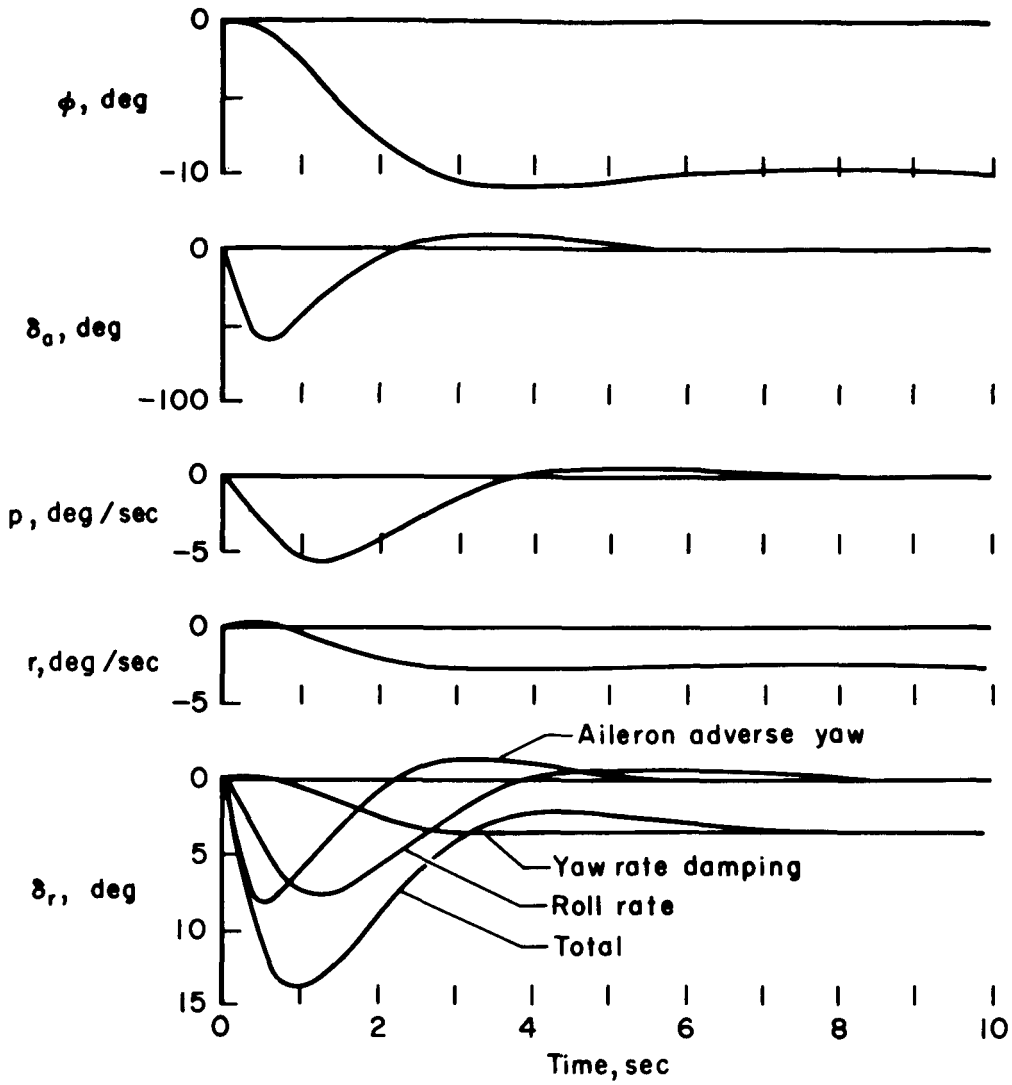

Figure 7.- Time history showing rudder requirements for a coordinated (β = 0) turn maneuver; V = 70 knots.

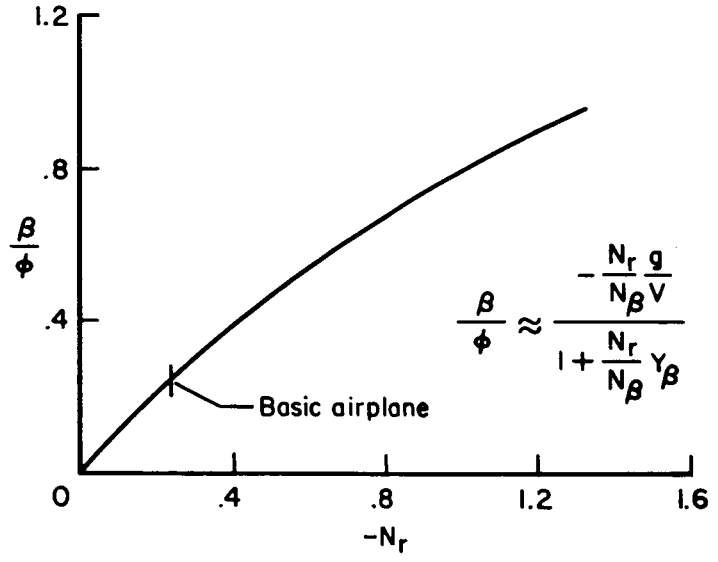

Figure 8.- Variation of ratio sideslip to bank angle in steady-state turn with rate damping.

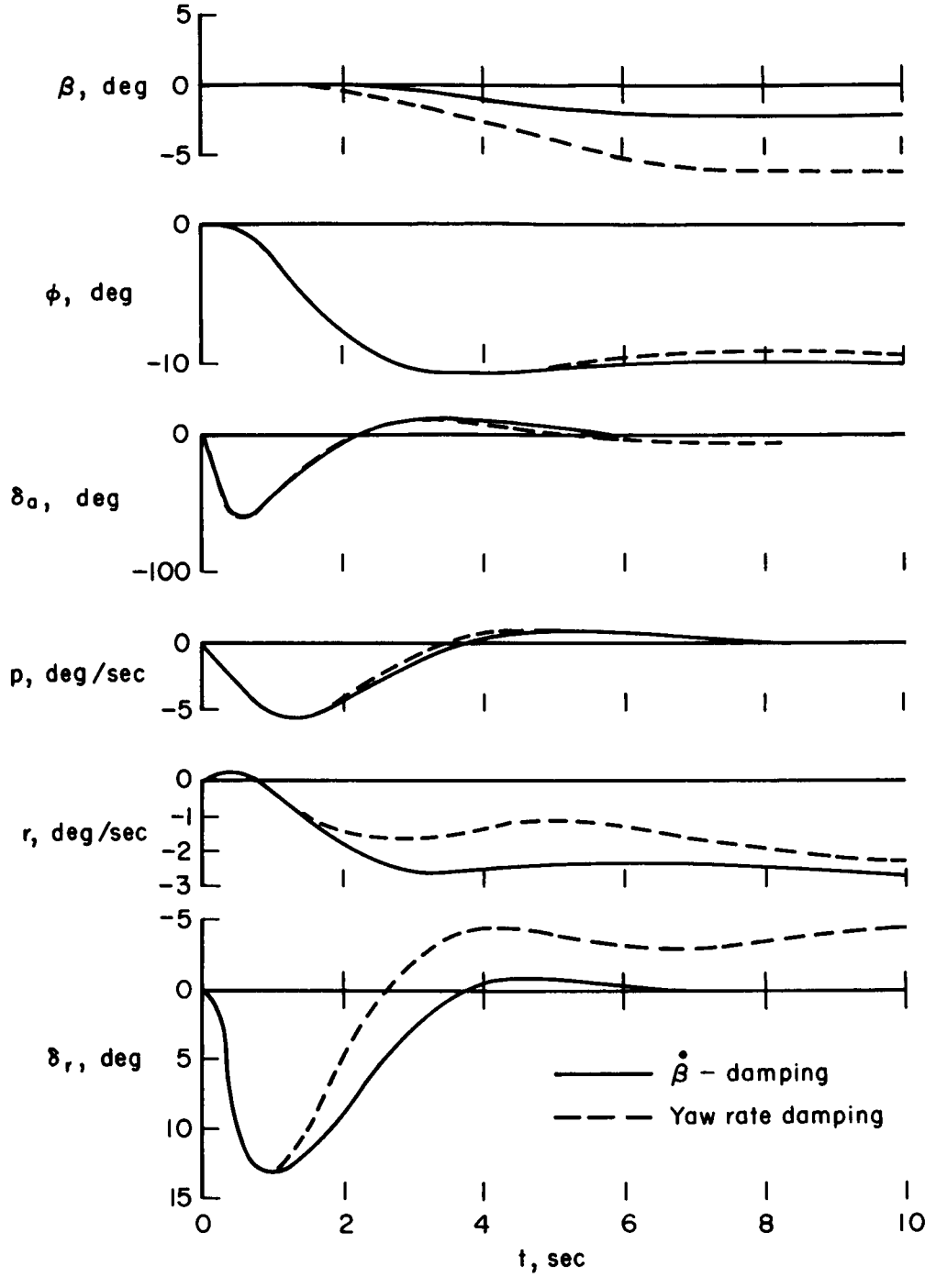

Figure 9.- A comparison of yaw rate and $\dot{\beta}$ damping in a turn entry; N_p = 0.27, V = 70 knots.

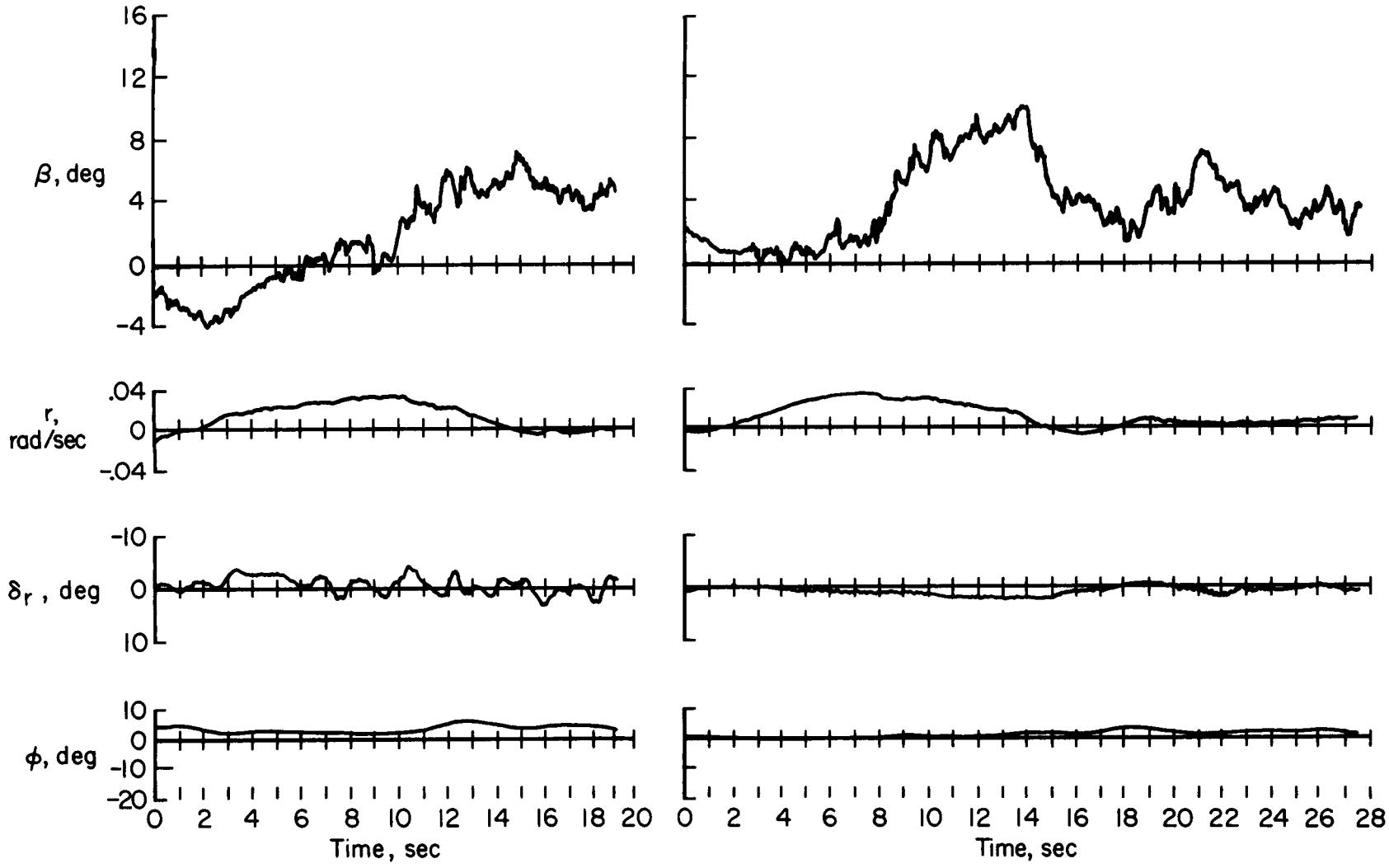

(a) Vane input.

(b) Airplane response input.

Figure 10.- Comparison of $\dot{\beta}$ damping in turbulence with two types of inputs; V ≈ 70 knots.

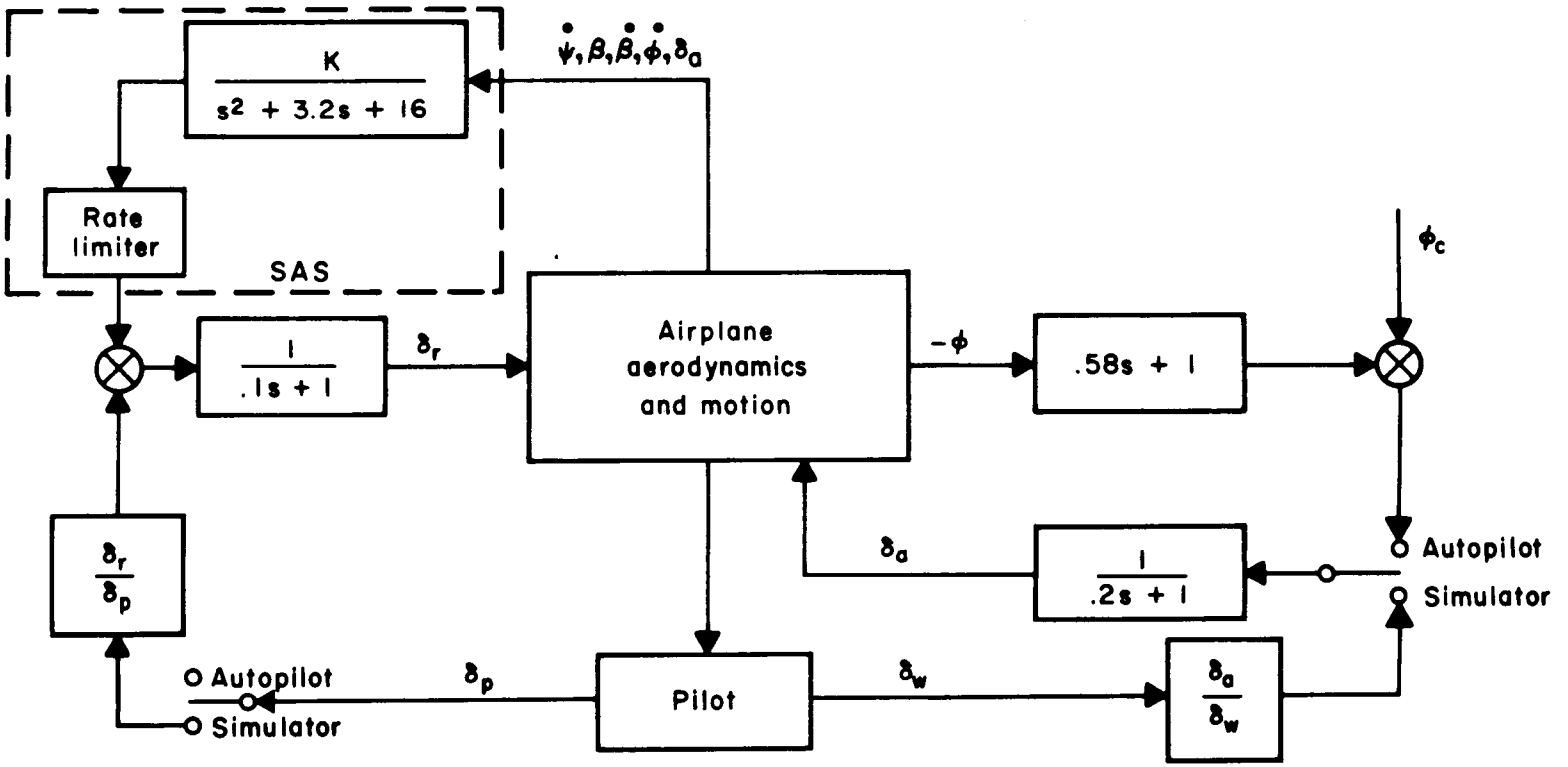

Figure 11.- Block diagram of simulated airplane with SAS.

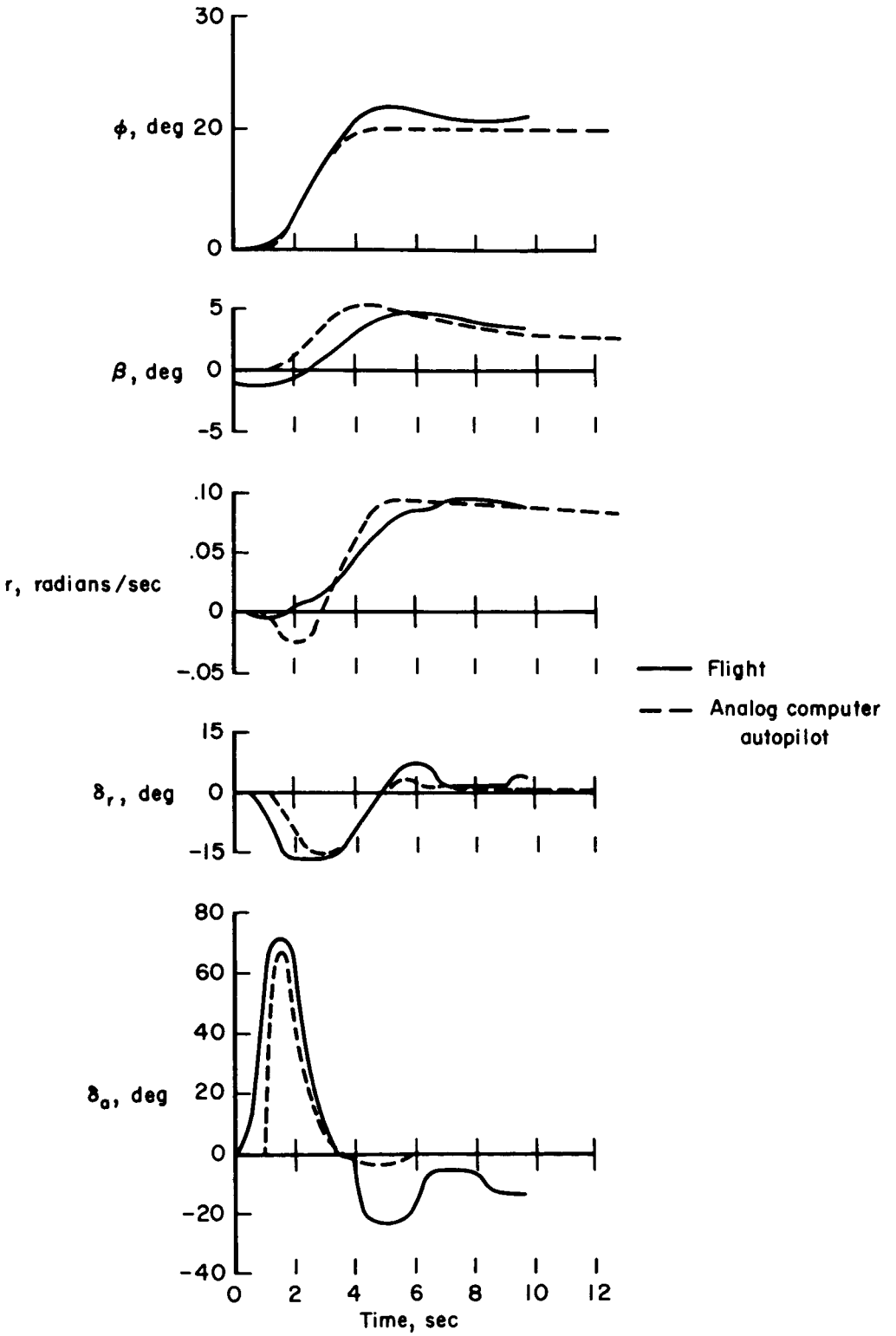

Figure 12.- A comparison of turn entry time history in flight with the analog computer autopilot.

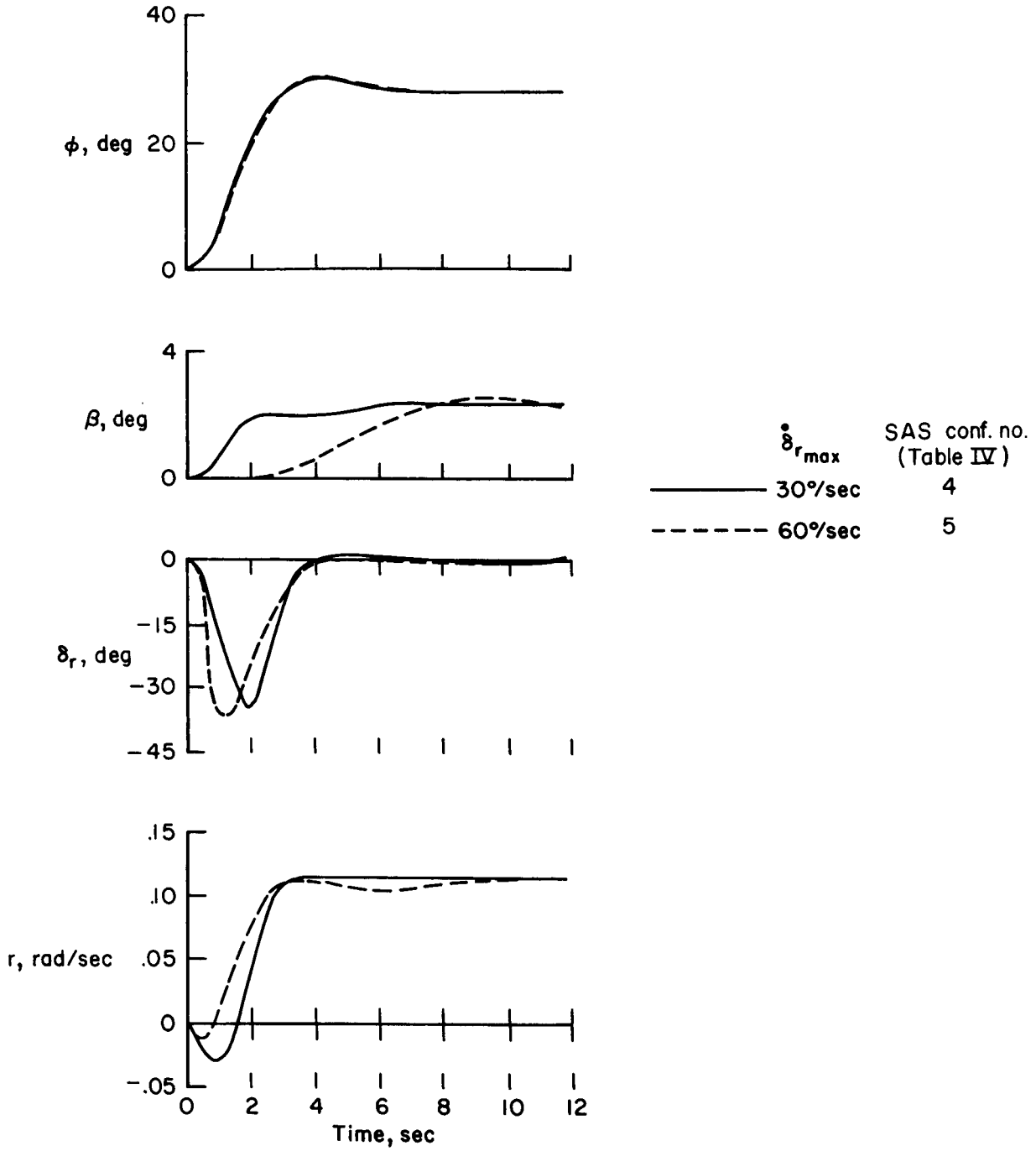

Figure 13.- A comparison of the sideslip phasing in a turn entry with two values of maximum rudder rate.

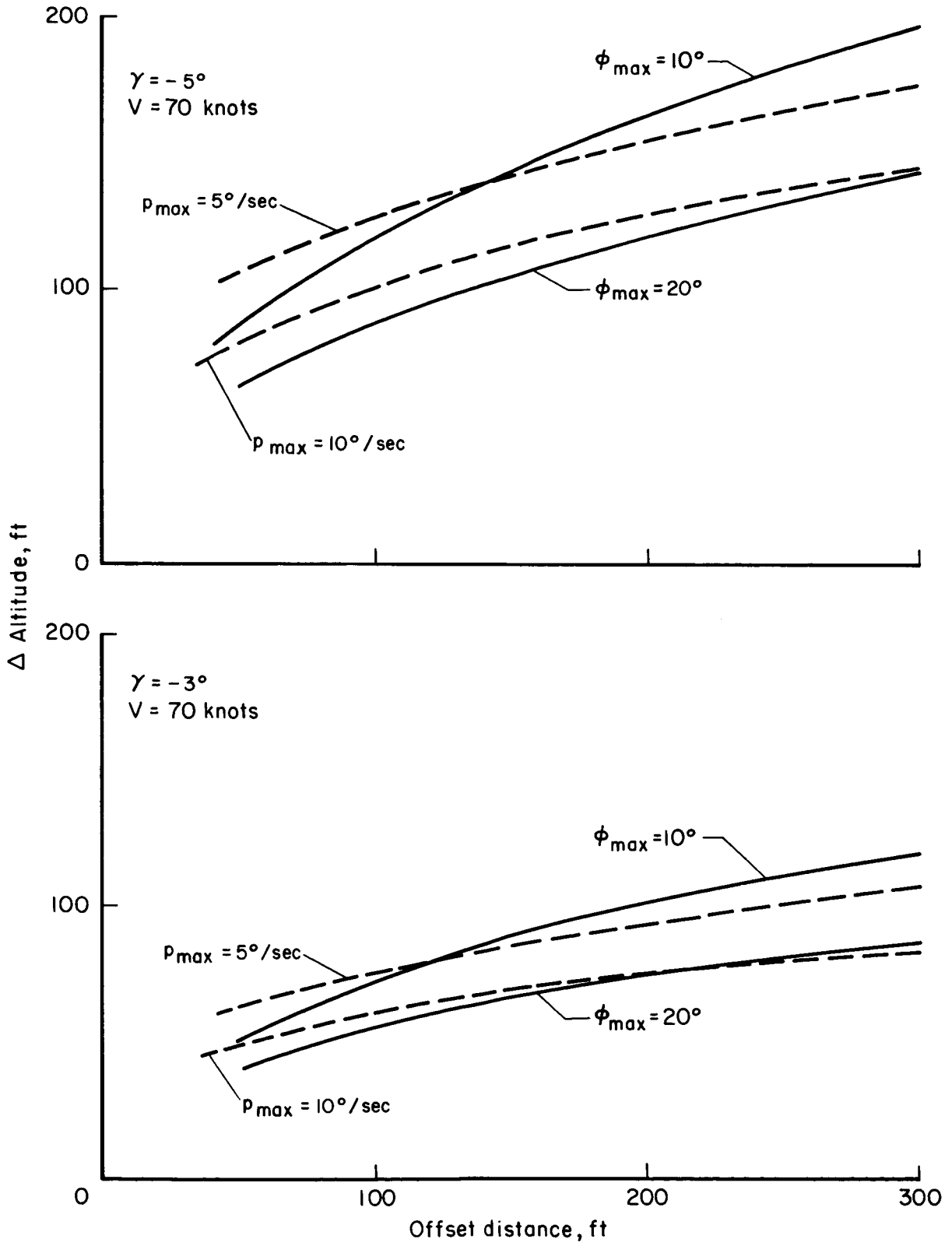

Figure 14.- Change in altitude to perform sinusoidal sidestep maneuver.